Poly(3,6-dihexyl-thieno[3,2-b]thiophene vinylene): Synthesis, Field-Effect Transistors, and Photovoltaic Properties

Youjun He,[†,‡] Weiping Wu,[†,‡] Guangjing Zhao,[†,‡] Yunqi Liu,*[,†] and Yongfang Li*[,†]

Beijing National Laboratory for Molecular Sciences, CAS Key Laboratory of Organic Solids, Institute of Chemistry, Chinese Academy of Sciences, Beijing 100190, China, and Graduate University of the Chinese Academy of Sciences, Beijing 100039, China

Received August 25, 2008; Revised Manuscript Received October 27, 2008

ABSTRACT: Poly(3,6-dihexyl-thieno[3,2-b]thiophene vinylene) (DH-PTTV) was prepared by the Pd-catalyzed Stille-coupling method. Compared with poly(3-hexylthienylene vinylene) (P3HTV), strong photoluminescence was observed for DH-PTTV solution, whereas the maximum absorption of DH-PTTV was blue-shifted. The solution-processed organic field-effect transistors (OFETs) were fabricated with bottom gate/top contact geometry. The highest FET hole mobility of DH-PTTV after thermal annealing at 180 °C for 30 min reached 0.032 $cm^2/V \cdot s$ with an on/off ratio of 10^5, which is a high value for the conjugated polymers. Polymer solar cells based on the polymers were fabricated, and the power conversion efficiency of the devices based on P3HTV and DH-PTTV was 0.19 and 0.28%, respectively, under the illumination of AM 1.5 and 100 mW/cm^2. The efficiency of the device based on DH-PTTV is ca. 50% higher than that of the devices based on P3HTV, which could be benefited from the higher hole mobility of DH-PTTV.

Introduction

In the past decades, conjugated organic and polymer materials have been the focus of great research activity, mainly because of their interesting electronic and optoelectronic properties. They are being investigated for a variety of applications, including organic field-effect transistors (OFETs),[1−4] organic light-emitting diodes (OLEDs), polymer solar cells (PSCs), and so on.[5−7] Poly(thienylene vinylene)s (PTVs) are an important class of the conjugated polymers. PTVs possess smaller bandgap (below 1.8 eV)[8,9] than do polythiophene (PT) derivatives[10] and higher hole mobility (10^{-4} to 10^{-2} $cm^2/V \cdot s$ measured in FET geometry).[11−15] The high hole mobility is a prerequisite for the applications in OFETs and PSCs. The smaller bandgap of PTVs makes their absorption spectra red-shifted and match well with the solar spectrum, which is also attractive for their application as photovoltaic polymers. However, at present, the power conversion efficiency (PCE) of the PSCs based on PTVs is quite low[16−18] because of the nonluminescent characteristic of PTVs. Obviously, the structure modification of PTVs could be an efficient way to look for new conjugated polymers of applications in OFETs and PSCs.

Polymers of fused thiophenes show higher hole mobility because of good π stacking in the solid state, so many polymers containing fused thiophene rings were synthesized and used in OFETs.[19−21] However, fused thiophene oligomers usually display poor solubility at room temperature; indeed, polymers of thieno[3,2-b]thiophenes are less soluble to preclude them from full characterization and utilization in devices.[22−24] Here we designed and synthesized a novel conjugated polymer of poly(3,6-dihexyl-thieno[3,2-b]thiophene vinylene) (DH-PTTV), as shown in Scheme 1, for modifying the structure of PTVs and for utilizing the advantage of fused thiophenes. The two hexyl groups on the thieno[3,2-b]thiophene units are for improving the solubility of the polymer because the two nonyl groups on polythieno[3,2-b]thiophene synthesized by Miguel et al.[25] OFETs and PSCs on the basis of the polymer were fabricated and characterized. The highest FET hole mobility of DH-PTTV after thermal annealing at 180 °C for 30 min reached 0.032 $cm^2/V \cdot s$ with an on/off ratio of 10^5. The PCE of the PSCs based on P3HTV and DH-PTTV was 0.19 and 0.28%, respectively, under the illumination of AM 1.5 and 100 mW/cm^2. The efficiency of the device based on DH-PTTV is ca. 50% higher than that of the device based on P3HTV, and it benefited from the higher hole mobility of DH-PTTV.

Scheme 1. Molecular Structures of the Polymers

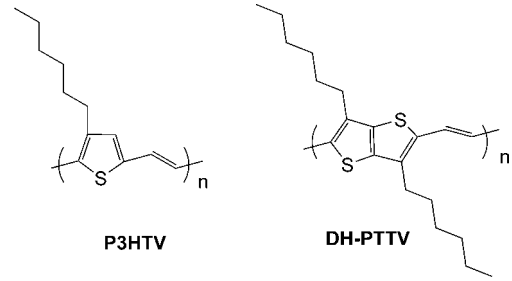

Results and Discussion

Synthesis of Monomers and Polymers. The synthesis routes of monomers and corresponding polymers are outlined in Schemes 2 and 3, respectively. P3HTV and DH-PTTV were prepared by Stille-coupling reaction[26] and confirmed by ^1H NMR spectroscopy and elemental analysis.

In the ^1H NMR spectrum of Compound **9** (Figure 1), the α-hydrogen linked to the thieno[3,2-b]thiophene of compound **9** peaks at 2.67 ppm; the other hydrogen positions are analyzed as shown in Figure 1. Figure 2 shows the ^1H NMR spectrum of DH-PTTV, where the double-bond hydrogen 7 and 8 correspond to the peaks in the range from 6.99 to 7.15 ppm. The α-hydrogen linked to the thieno[3,2-b]thiophene of DH-PTTV positions at 2.79 ppm.

DH-PTTV is soluble in common organic solvents, such as chloroform, toluene, and THF at room temperature. The elemental analysis, weight-average molecular weight (M_w) and polydispersity index (PDI) of the polymers are shown in Table 1.

* Corresponding authors. E-mail: liyf@iccas.ac.cn (Y. F. Li); liuyq@iccas.ac.cn (Y. Q. Liu).
† Institute of Chemistry.
‡ Graduate University.

10.1021/ma801923c CCC: $40.75
Published on Web 11/19/2008

Scheme 2. Synthesis Routes of the Monomers[a]

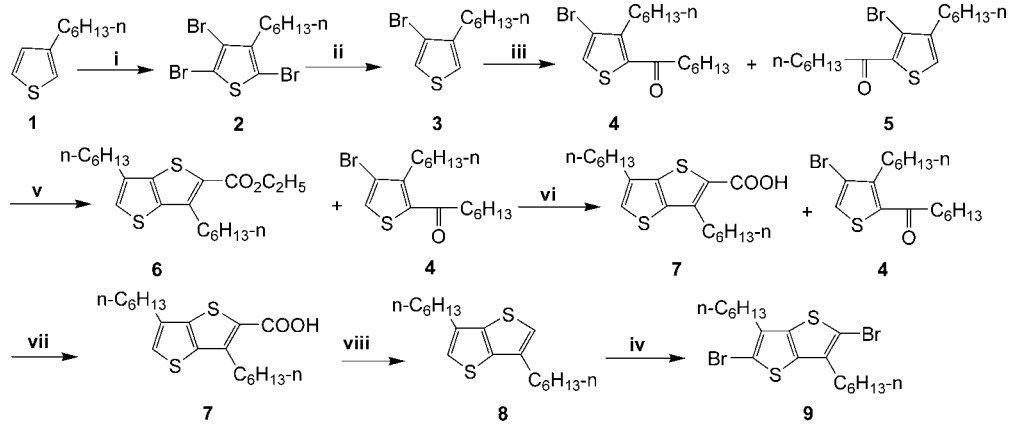

[a] (i) Br_2, HOAc, 4 h, then 60−70 °C, 24 h; (ii) butyl lithium, THF, −78 °C, 1 h, then H_2O; (iii) $AlCl_3$, $C_6H_{13}COCl$, CH_2Cl_2, room temperature, 2 h; (v) $HSCOOC_2H_5$, K_2CO_3, 18-crown-ether, 60 °C, 24 h; (vi) THF/CH_3OH, LiOH, tetrabutylammonium iodide, reflux, 24 h; (vii) separate by column chromatography; (viii) Cu, quinoline, 260 °C, 4 h; (iv) NBS, DMF, room temperature, 24 h.

Scheme 3. Synthesis Routes of the Polymers[a]

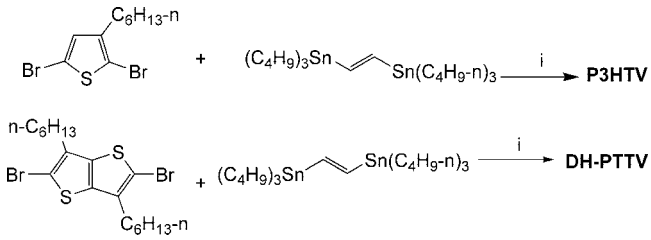

[a] (i) Pd $(PPh_3)_4$, toluene, argon, reflux, 12 h.

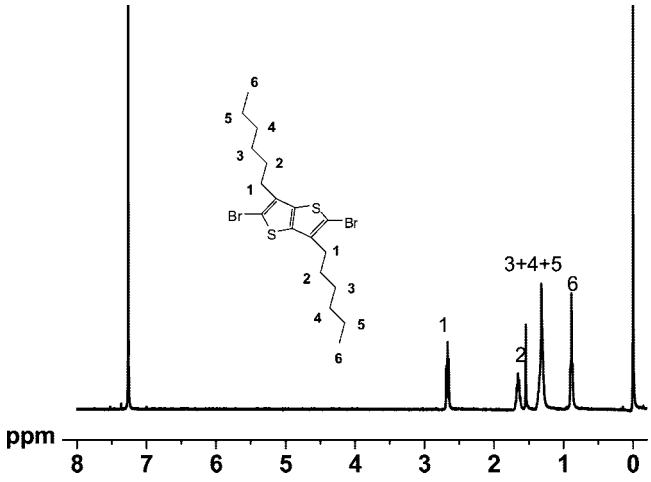

Figure 1. ^{1}H NMR spectra of compound **9**.

Thermal Analysis. The thermal stability of the polymers was investigated with thermogravimetric analysis (TGA), as shown in Figure 3a. P3HTV and DH-PTTV show onset decomposition temperatures with 5% weight loss at 350 and 314 °C, respectively, which was also listed in Table 1. The thermal stability is enough for most applications.

The thermally induced phase-transition behavior of P3HTV and DH-PTTV was investigated with differential scanning calorimetry (DSC), as shown in Figure 3b. The glass-transition temperatures (T_g) of the polymers obtained by DSC were 64.5 and 125 °C for P3HTV and DH-PTTV, respectively. It is obvious that the incorporation of fused thiophene moiety increases the T_g value, which is possibly due to reduced segmental motions as well as denser packing in polymer main chains.

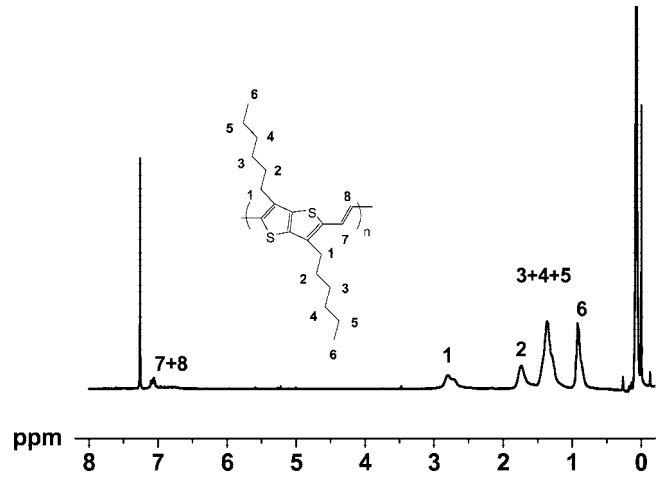

Figure 2. ^{1}H NMR spectra of polymer DH-PTTV.

Table 1. Elemental Analysis, Weight-Average Molecular Weight, and TGA Properties of the Polymers

	elemental analysis: calcd/found (%)			molecular weight by GPC		
polymers	C	H	S	M_w[a]	PDI	T_{5d} (°C)[b]
P3HTV	75.00/74.36	8.33/8.21	16.66/14.98	28K	3.08	350
DH-PTVV	72.29/72.18	8.43/8.72	19.28/18.96	32K	1.13	314

[a] Weight-average molecular weight determined by GPC using polystyrene as the standard in THF solution. [b] Decomposition temperature determined by TGA in N_2 atmosphere at 5% weight loss.

Optical Properties of the Polymers. Figure 4 shows the absorption spectra of the polymer solutions in chloroform and films on quartz plates. The absorption peak of DH-PTTV solution centered at 538 nm, which is about 18 nm blue-shifted in comparison with that of P3HTV, as shown in Figure 4a. This blue shift of the absorption spectra of DH-PTTV could result from the rigid structure of the fused thiophene rings in the polymers. The steric repulsion between β-alkyl chains probably prevents the coplanarity of ring units and causes a decrease in the effective conjugation length of the polymer chain in DH-PTTV.

Figure 4b shows the absorption spectra of the polymer films on quartz plates. The absorption peaks of P3HTV and DH-PTTV films are located at 580 and 542 nm, respectively. The

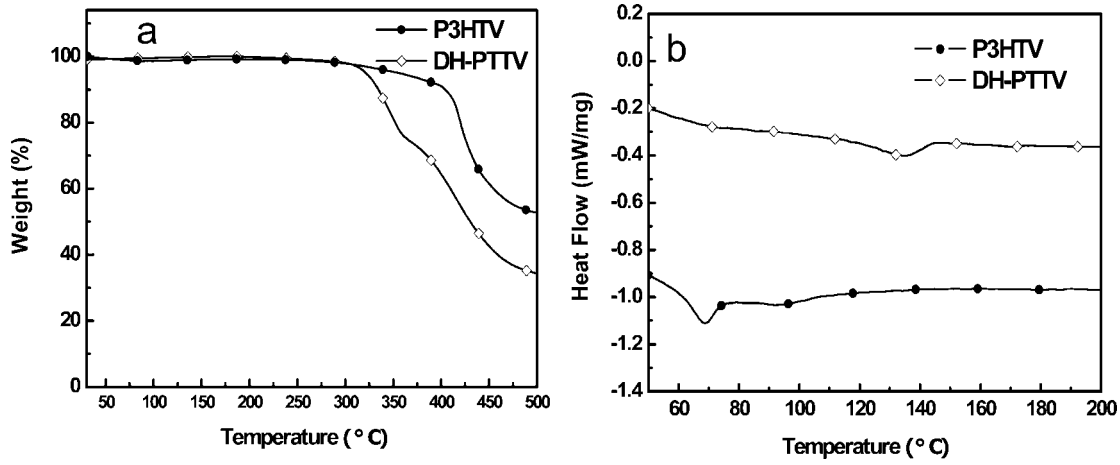

Figure 3. (a) TGA plots of P3HTV and DH-PTTV with a heating rate of 10 °C/min under an inert atmosphere. (b) DSC thermogram of P3HTV and DH-PTTV.

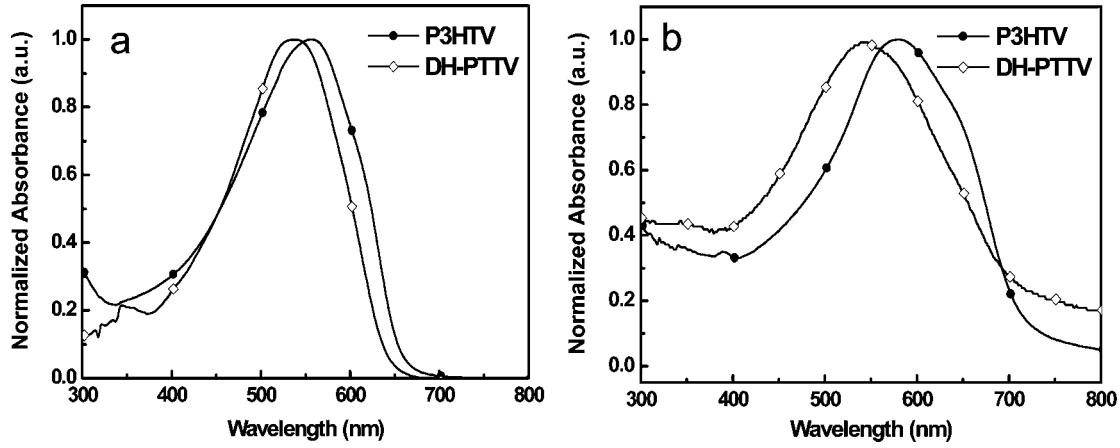

Figure 4. Normalized absorption spectra of the polymers: (a) solutions in chloroform and (b) films spin-coated on quartz plates.

Table 2. Absorption Spectral Properties of P3HTV and DH-PTTV

polymers	λ_{max} (nm) in solutions	λ_{max} (nm) in films	λ_{edge} (nm) in films
P3HTV	556	580	712
DH-PTTV	538	542	700

absorption peaks of P3HTV and DH-PTTV films are red-shifted relative to those of their solutions by 24 and 4 nm, respectively, which results from the interchain interactions in the polymer films. The absorption peaks and edge wavelengths of the polymers are outlined in Table 2.

Interestingly, DH-PTTV shows strong photoluminescence (PL) in the wavelength range from 500 to 750 nm (peaks at ca. 650 nm), whereas no PL emission can be observed for P3HTV, as shown in Figure 5. It is well known that poly(thienylene vinylene) is a nonluminescent polymer.[16] The strong PL spectrum of DH-PTTV indicates that the fused thiophene units in the polymers greatly influence the optical properties of the polymers.

Electrochemical Properties. The electrochemical property is one of the most important properties of the conjugated polymers, and many applications of the conjugated polymers depend on the electrochemical properties. We studied the redox potentials of the polymers by cyclic voltammetry (CV).

Figure 6 shows the cyclic voltammograms of the polymer films on the Pt electrode. It can be seen that they exhibit *p*-doping/dedoping (oxidation/re-reduction) processes at positive potential range and *n*-doping/dedoping (reduction/reoxidation) processes at negative potential range.

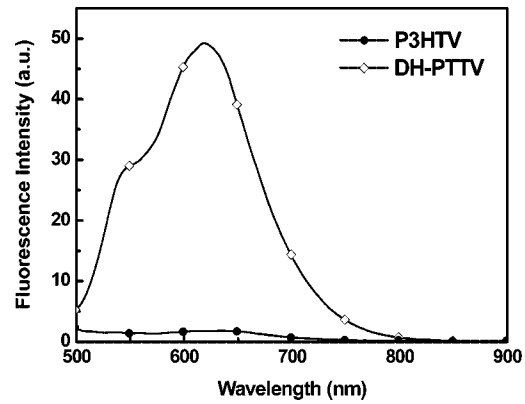

Figure 5. Photoluminescence spectra of the polymer solutions in chloroform (concentration 10^{-5} M).

The HOMO and LUMO energy levels of the polymers are calculated from the onset oxidation potentials (φ_{ox}) and the onset reduction potentials (φ_{red}) and by assuming the energy level of ferrocene/ferrocenium (Fc/Fc^+) to be -4.8 eV below the vacuum level.[27] The formal potential of Fc/Fc^+ was measured to be 0.09 V against Ag/Ag^+. The energy gap (E_g stack) of the polymers was calculated from the HOMO and LUMO energy levels. The calculating equations are as follows[28]

$$E_{HOMO} = -e(\varphi_{ox} - \varphi_{Fe/Fe^+} + 4.8) \quad (eV)$$

$$E_{LUMO} = -e(\varphi_{red} - \varphi_{Fe/Fe^+} + 4.8) \quad (eV)$$

$$E_g^{ec} = e(\varphi_{ox} - \varphi_{red}) \quad (eV)$$

where the units of φ_{ox} and φ_{red} are V versus Ag/Ag^+. The value of φ_{Fc/Fc^+} is 0.09 V. The values obtained are listed in Table 3. The φ_{ox} of DH-PTTV is positively shifted by 0.12 V compared with P3HTV, but the value of φ_{red} is negatively shifted by 0.01 V compared with P3HTV. The electrochemical energy gap of DH-PTTV is larger than that of P3HTV by 0.13 eV.

Field-Effect Transistor Properties of the Polymers. Figure 7 shows the typical output and transfer curves of a representative OFET device with DH-PTTV as the active layer. The device performances of the two polymers are summarized in Table 4. The output behavior closely followed the metal-oxide semiconductor FET gradual-channel model with very good saturation and no observable contact resistance (Figure 7a,c).

The transfer characteristics of DH-PTTV show very low conductivity at zero gate voltage (Figure 7b), which shows its high air stability due to the low HOMO (−5.04 eV) energy level. Without annealing, the OFET with DH-PTTV as the active layer showed a mobility of 4.64×10^{-4} $cm^2/V \cdot s$ in the saturation regime, together with an on/off ratio of 10^3 when measured under ambient conditions. Annealing the devices at 150 and 180 °C for 30 min led to improved charge carrier mobilities of up to 7.54×10^{-3} and 0.019 $cm^2/V \cdot s$, respectively. The highest mobility of DH-PTTV reached 0.032 $cm^2/V \cdot s$ with an on/off ratio of 10^5 and a threshold voltage of −14.2 V. The on/off ratio increased to 10^4 to 10^5 (the highest on/off ratio is 7.2×10^5) because of the increased drain current and low current at zero gate voltage (below 10^{-9} A). With low HOMO (−4.92 eV) energy level, P3HTV also showed very high air stability despite its relatively low mobility (on the order of 10^{-4} $cm^2/V \cdot s$ with a threshold voltage of −8.4 V), which is in sharp contrast with that of most polymer semiconductors such as P3HT and its analogues.

Atomic force microscopy (AFM) was used to observe surface morphologies of the polymer films to understand the effect of thermal annealing on the mobility of the polymers. The AFM images of both the unannealed and annealed P3HTV films exhibited typical amorphous morphology without any crystalline domains, as shown in Figure 8a,b. Moreover, P3HTV films spin-coated onto the dielectric surface got depressions in some regions, which may have a negative effect on the charge transport. It can be seen from Figure 8c that the morphology of the DH-PTTV film before annealing is also amorphous. But, the thermal annealing of DH-PTTV film at 180 °C induced the morphology with crystalline domains, as shown in Figure 8d. The effect of the thermal annealing on the morphology of the polymer films could be the reason in which the mobility of P3HTV was not improved after annealing whereas that of DH-PTTV was remarkably increased.

Photovoltaic Properties of the Polymers. The motivation of the design and synthesis of the polymer DH-PTTV is to look for novel poly(thiophene vinylene) derivatives used in PSCs. We fabricate the PSCs with the structure of ITO−PEDOT-PSS−polymer/PCBM (1:1 w/w)−Ca−Al, where the polymer (P3HTV or DH-PTTV) was used as the electron donor and PCBM was used as the electron acceptor.

Figure 9 shows the *I* versus *V* curves of the PSCs under the illumination of AM 1.5 and 100 mW/cm^2, and Table 5 lists the photovoltaic properties obtained from the *I* versus *V* curves for the best devices. The V_{oc} of the device based on DH-PTTV increased by 0.06 V compared with that of P3HTV and benefited from the lower HOMO energy level of DH-PTTV than that of P3HTV. The PCE of the devices based on DH-PTTV reached 0.28%, which is ca. 50% greater than that of the device based on P3HTV. The higher short circuit current and higher efficiency of the PSC based on DH-PTTV could be ascribed to the higher hole mobility of DH-PTTV.

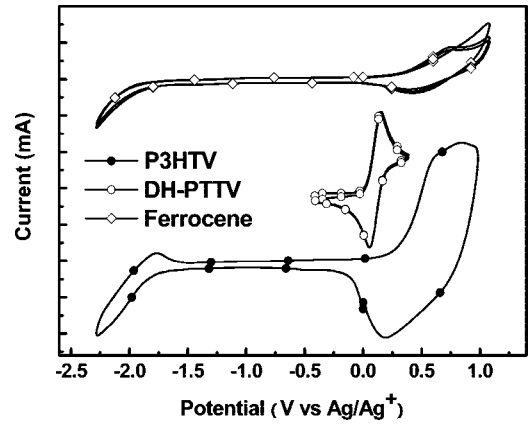

Figure 6. Cyclic voltammograms of the polymer films on Pt electrode infilms on Pt electrode 0.1 mol/L Bu_4NPF_6, CH_3CN solution with a scan rate of 100 mV/s.

Table 3. Electrochemical Onset Potentials and Electronic Energy Levels of the Polymer Films

polymers	φ_{ox} (V vs Ag/Ag^+)/E_{HOMO} (eV)	φ_{red} (V vs Ag/Ag^+)/E_{LUMO} (eV)	E_g^{ec} (eV)	E_g^{opt} (eV)[a]
P3HTV	0.21/−4.92	−1.73/−2.98	1.94	1.74
DH-PTTV	0.33/−5.04	−1.74/−2.97	2.07	1.77

[a] Optical band gap was obtained from empirical formula, $E_g^{opt} = 1240/\lambda_{edge}$, in which λ_{edge} is the onset wavelength of its absorption peak in the longer wavelength direction.

Conclusions

DH-PTTV was prepared by the Pd-catalyzed Stille-coupling method. Compared with P3HTV, the absorption peak of DH-PTTV is slightly blue-shifted, whereas the PL intensity of DH-PTTV solution was greatly enhanced. The solution-processed polymer OFETs were fabricated with bottom gate/top contact geometry and were characterized. The as-prepared OFET with DH-PTTV as the active layer showed a hole mobility of 4.64×10^{-4} $cm^2/V \cdot s$ together with an on/off ratio of 10^3. Annealing the devices at 150 and 180 °C for 30 min greatly increased the hole mobilities up to 7.54×10^{-3} and 0.019 $cm^2/V \cdot s$, respectively. The highest hole mobility of DH-PTTV reached 0.032 $cm^2/V \cdot s$ with an on/off ratio of 10^5. The PCE of the PSCs based on P3HTV and DH-PTTV was 0.19 and 0.28%, respectively. The PCE of the device based on DH-PTTV was ca. 50% greater than that of the device based on P3HTV, which could be ascribed to the higher hole mobility of DH-PTTV.

Experimental Section

Materials. 3-Bromo-thiophene, $Pd(PPh_3)_4$, bromine, tributyltin chloride, NBS, *n*-butyllithium (2.88 mol/L in hexane), heptanoyl chloride, ethyl mercaptoacetate, K_2CO_3, DMF, 18-crown-ether, LiOH, tetrabutylammonium iodide, copper powder, quinoline, bromobenzene, and benzene boronic acid were obtained from Acros Organics. Tetrahydrofuran (THF) was dried over Na/benzophenone ketyl and freshly distilled prior to use. The monomer 2,5-dibromo-3-hexylthiophene for the synthesis of P3HTV was synthesized as reported in the literature.[26] (*E*)-1,2-bis (tributylstannyl)ethane was synthesized as reported in the literature.[17] Other materials were common commercial level and were used as received.

Measurement and Characterization. General Methods: All new compounds were characterized by ^1H NMR. Nuclear magnetic resonance (NMR) spectra were taken on a Bruker DMX-400 spectrometer. Chemical shifts of ^1H NMR were reported in ppm relative to the singlet at 7.26 ppm. Splitting patterns were designated as s (singlet), t (triplet), d (doublet), m (multiplet), and br (broaden).

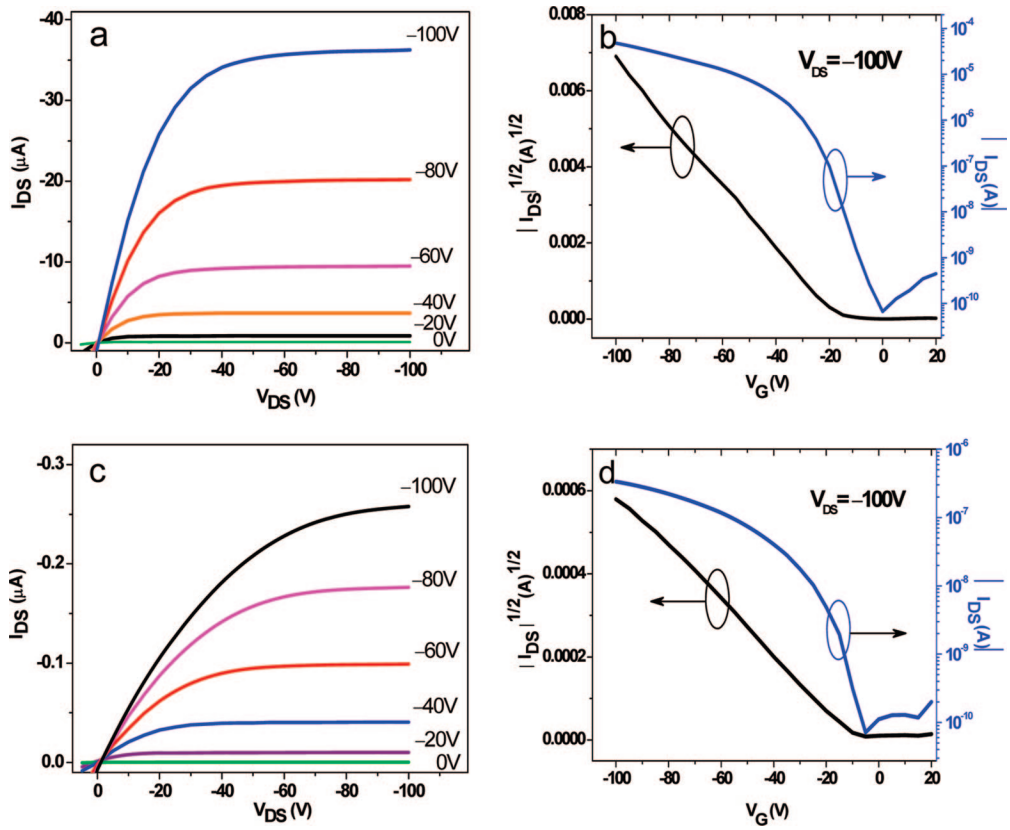

Figure 7. (a) Output and (b) transfer characteristics of top-contact OFETs using DH-PTTV as the active layer. (c) Output and (d) transfer characteristics of top-contact OFETs using P3HTV as the active layer. I_{DS} was obtained at $V_{DS} = -100$ V for transfer characteristics.

Table 4. FET Properties of Devices with the Polymer Films Spin-Coated on OTS-Modified SiO_2/Si Substrates

			without annealing		annealed at 120 °C		annealed at 180 °C	
polymers	LUMO (eV)	HOMO (eV)	μ (cm^2/V·s)	I_{on}/I_{off}	μ (cm^2/V·s)	I_{on}/I_{off}	μ (cm^2/V·s)	I_{on}/I_{off}
P3HTV	−2.98	−4.92	2.02×10^{-4}	10^3	3.12×10^{-4}	10^3	3.76×10^{-4}	10^3−10^4
DH-PTTV	−2.97	−5.04	4.64×10^{-4}	10^3−10^4	7.54×10^{-3}	10^4−10^5	0.019	10^4−10^5

Absorption spectra were taken on a Hitachi U-3010 UV−vis spectrophotometer. PL spectra were measured using a Hitachi F-4500 spectrophotometer. Absorption and PL spectra measurements of the polymer solutions were carried out in chloroform (analytical reagent) at 25 °C. Absorption and PL spectra measurements of the polymer films were carried out on the quartz plates with the polymer films spin-coated from the polymer solutions in chloroform (analytical reagent) at 25 °C. The molecular weight of the polymers was measured by GPC method, and polystyrene was used as a standard. The TGA measurement was performed on a Perkin-Elmer TGA-7 apparatus. The electrochemical CV was conducted on a Zahner IM6e electrochemical workstation with a Pt disk, Pt plate, and Ag/Ag$^+$ electrode as the working electrode, counter electrode, and reference electrode, respectively, in a 0.1 mol/L tetrabutylammonium hexafluorophosphate (Bu_4NPF_6) acetonitrile solution. Polymer thin films were formed by drop-casting 1.0 mm^3 of polymer solutions in THF (analytical reagent, 1 mg/mL) on the working electrode and were then dried in air.

Fabrication of Field-Effect Transistor Devices. Thin-film OFETs were fabricated on highly doped silicon substrates with thermally grown 500-nm-thick silicon oxide (SiO_2) insulating layer (capacitance per unit area $C_i = 6$ nF/cm^2), where the substrate served as a common gate electrode. Prior to organic semiconductor deposition, the substrates were treated with the silylating agent octyltrichlorosilane (OTS). Thin semiconductor films were then deposited by spin-coating the polymer solutions in dichlorobenzene (1 wt %) on the substrates. The film thickness was ∼30 nm, as measured by an XP-2 surface profilometer (Ambios Technology). The samples were then dried and annealed at 120−180 °C under nitrogen for 30 min. Transistor source−drain gold electrodes were vacuum deposited on the polymer layer to form top-contact geometry (channel length, $L = 50$ μm, and channel width, $W = 3000$ μm). The electrical characterization of the transistor devices was performed using a Keithley 4200 semiconductor parameter analyzer.

Fabrication of Photovoltaic Devices. PSCs were fabricated with ITO glass as a positive electrode, Ca/Al as a negative electrode, and the blend film of the polymer/PCBM between them as a photosensitive layer. The ITO glass was precleaned and modified by a thin layer of PEDOT/PSS (Bayer), which was spin-cast from a PEDOT/PSS aqueous solution on the ITO substrate, and the thickness of the PEDOT/PSS layer was ∼60 nm. The photosensitive layer was prepared by spin-coating a blend solution of the polymer and PCBM with a weight ratio of 1:1 in *o*-dichlorobenzene at 1000 rpm on the ITO−PEDOT/PSS electrode. Then, the Ca/Al cathode was deposited on the polymer layer by vacuum evaporation under 3×10^{-4} Pa. The thickness of the photosensitive layer was ca.80 nm, measured on an Ambios Tech XP-2 profilometer. The effective area of one cell was ca. 4 mm^2. The current−voltage (*I* versus *V*) measurement of the devices was conducted on a computer-controlled Keithley 236 source measure unit. A xenon lamp with an AM 1.5 filter was used as the white-light source, and the optical power at the sample was ∼100 mW/cm^2.

Synthesis of the Monomers. *2,4,5-Tribromo-3-hexylthiophene (**2**).* 3-Hexylthiophene **1** (100.00 g, 0.60 mol) was mixed with 200 mL of acetic acid. To this mixture was added bromine (92.60 mL, 1.80 mol) dropwise. After the addition of bromine, the mixture was stirred at room temperature for 4 h and heated to 60−70 °C overnight. The final mixture was poured in 800 mL of ice water and neutralized with NaOH solution (6 mol/L). The organic was

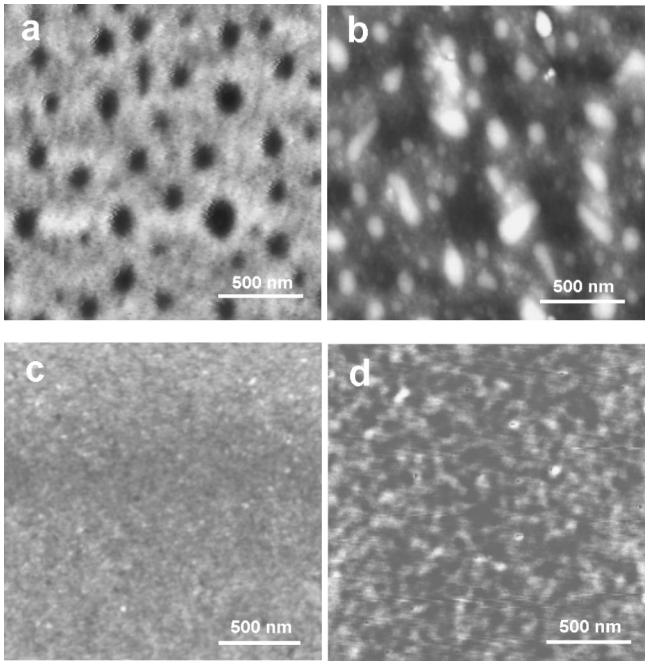

Figure 8. AFM images of P3HTV film (a) before thermal annealing and (b) after thermal annealing at 180 °C for 30 min and of DH-PTTV film (c) before thermal annealing, and (d) after thermal annealing at 180 °C for 30 min. (scale: 2 × 2 μm^2).

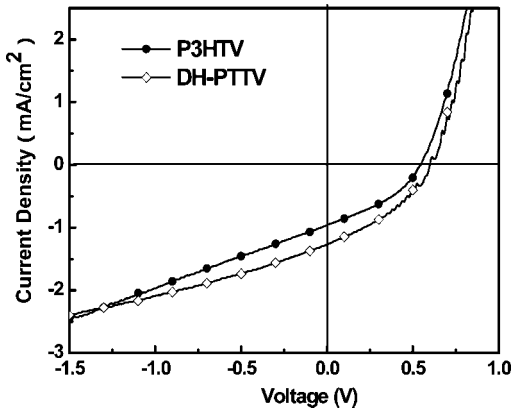

Figure 9. *I* versus *V* curves of the PSCs based on the polymers under the illumination of AM 1.5 and 100 mW/cm^2.

Table 5. Photovoltaic Properties of the PSCs under the Illumination of AM 1.5, 100 mW/cm^2

polymers	V_{oc} (V)	I_{sc} (mA/cm^2)	FF	HOMO (eV)	LUMO (eV)	PCE
P3HTV	0.54	0.96	0.37	−4.92	−2.98	0.19%
DH-PTTV	0.60	1.27	0.37	−5.04	−2.97	0.28%

extracted with ethyl acetate (3 × 100 mL). The combined organic was washed with brine (2 × 100 mL) and water (100 mL) and was dried over anhydrous $MgSO_4$. After the solvent was evaporated, 234.00 g (96.5%) of crude product **2** was obtained. This product was found to be good enough for the next reaction. GC/MS: 404 (M-1). ^{1}H NMR ($CDCl_3$, 400 MHz, δ): 2.64 (t, 2H), 1.51 (m, 2H), 1.32 (m, 6H), 0.89 (t, 3H). ^{13}C NMR (300 MHz, CD_2Cl_2): 143.7, 117.9, 111.5, 110.2, 33.6, 32.9, 31.00, 30.5, 24.7, 16.0. Anal. Calcd for $C_{10}H_{13}SBr_3$: C, 29.63; H, 3.21; S, 7.90; Br, 59.26. Found: C, 29.55; H, 3.13; S, 7.76; Br, 59.23.

*3-Bromo-4-hexylthiophene (**3**).* Compound **2** (70.00 g, 0.17 mol) was mixed with dry THF (400 mL). To this mixture was added *n*-butyllithium (138 mL, 2.5 M in hexane, 0.35 mol) dropwise at −78 °C under argon. After the addition was finished, the mixture was stirred for another 10 min, and water was added to quench the reaction. The THF was evaporated, and the organic was extracted with ethyl acetate (2 × 100 mL). The combined organic layer was washed by brine (2 × 100 mL) and water (70 mL) and was dried over anhydrous $MgSO_4$. After the solvent was evaporated, the crude product was purified by vacuum distillation at 136 °C under 0.20 mbar to give the product of **3** (35.30 g, 84.1%). GC/MS: 246(M-1). ^{1}H NMR ($CDCl_3$, 400 MHz, δ): 7.22 (s, 1H), 6.96 (s, 1H), 2.57 (t, 2H), 1.61 (m, 2H), 1.32 (m, 6H), 0.88 (t, 3H). ^{13}C NMR (300 MHz, CD_2Cl_2): 141.9, 122.9, 121.0, 112.9, 31.9, 30.1, 29.5, 29.2, 22.9, 14.1. Anal. Calcd for $C_{10}H_{15}SBr$: C, 48.58; H, 6.07; S, 12.96; Br, 32.39. Found: C, 48.49; H, 5.92; S, 12.88; Br, 32.30.

*1-(3-Bromo-4-hexyl-2-thienyl)heptanone (**5**).* To a mixture of compound **3** (24.70 g, 0.10 mol) and $AlCl_3$ (26.80 g, 0.20 mol) in dry CH_2Cl_2 (100 mL) was added heptanoyl chloride (14.90 g, 0.10 mol) dropwise at room temperature. This mixture was stirred for 2 h and was then analyzed by GC/MS to be a 3:1 mixture of target compound **5** and heptanone **4**. The mixture was poured in HCl (6 mol/L) and was washed three times with water (50 mL). The organic mixture then was dried over anhydrous $MgSO_4$. After the solvent was evaporated, 34.70 g of the **4** and **5** mixture of crude products was obtained, as confirmed by GC/MS, and was used for the next reaction without separation.

*3,6-Dihexyl-thieno[3,2-b]thiophene-2-carboxylic Acid (**7**).* The mixture of compounds **4** and **5** (66.50 g, 0.19 mol) was mixed with K_2CO_3 (53.60 g, 0.39 mol) and a catalytic amount of 18-crown-6 in 200 mL of DMF. To this mixture was added ethyl mercaptoacetate (20.30 mL, 0.19 mol) dropwise at 60−70 °C. The mixture was stirred at this temperature overnight and was poured in water (800 mL). The organic was extracted with ethyl acetate (3 × 100 mL) and was washed with brine (2 × 100 mL) and water (100 mL). The organic layer was collected, and the solvent was evaporated. The residue included 3,6-dihexyl-thieno[3, 2-b]thiophene-2-carboxylic acetate **6** and compound **4**, as confirmed by GC/MS. This mixture was then dissolved in THF (300 mL). To this THF solution were added LiOH (84 mL, 10% w/w solution in water), MeOH (50 mL), and a catalytic amount of tetrabutylammonium iodide. The mixture was refluxed for 3 h, and the solvent then was evaporated. The residue was acidified with concentrated HCl (50 mL). The organic was extracted with ethyl acetate (3 × 100 mL) after dilution by water. The combined organic layer was washed with brine (2 × 100 mL) and water (100 mL) and was dried over anhydrous $MgSO_4$. After the solvent was evaporated, compound **7** was obtained by silica gel column chromatography (5% ethyl acetate in hexane and then 20% ethyl acetate in hexane to elute). Yield: 30.00 g (44.9%) (calculated from mixture). EI *m/z*: = 352. ^{1}H NMR ($CDCl_3$, 400 MHz, δ): 7.24 (s, 1H), 3.18 (t, 2H), 2.73 (t, 2H), 1.75 (m, 4H), 1.34 (m, 14H), 0.89 (m, 6H). ^{13}C NMR (300 MHz, CD_2Cl_2): 169.2, 146.3, 143.1, 141.5, 136.1, 126.7, 126.1, 32.0, 29.7 (6C), 23.0, 14.2. Anal. Calcd for $C_{19}H_{28}S_2O_2$: C, 64.77; H, 7.95; S, 18.18; O, 9.09. Found: C, 64.56; H, 7.88; S, 18.12; O, 8.89.

*3,6-Dihexyl-thieno[3,2-b]thiophene (**8**).* A solution of compound **7** (30.00 g, 0.09 mol), copper powder (3.76 g), and quinoline (80 mL) was heated to 260 °C in a Wood's metal bath. After refluxing for 4 h, the mixture was cooled to room temperature, and hexane (200 mL) was added to the quinoline mixture. This mixture was washed repeatedly with 1 mol/L HCl. The organic layer was dried over anhydrous $MgSO_4$, and the solvent was removed. Compound **8** was obtained after silica gel chromatography. Light petroleum eluted **8** (18.00 g, 68.8%). EI *m/z*: = 308. mp 58−59 °C. ^{1}H NMR ($CDCl_3$, 400 MHz, δ): 6.97 (s, 2H), 2.70 (t, 4H), 1.73 (m, 4H), 1.37 (m, 12H), 0.88 (t, 6H). ^{13}C NMR (300 MHz, CD_2Cl_2): 136.6, 135.0, 109.8, 31.9, 29.3, 29.3, 28.5, 23.0, 14.2. Anal. Calcd for $C_{18}H_{28}S_2$: C, 70.13; H, 9.09; S, 20.78. Found: C, 70.08; H, 9.03; S, 20.56.

*2,5-Dibromo-3,6-dihexyl-thieno[3, 2-b]thiophene (**9**).* Compound **8** (18.00 g, 0.06 mol) was dissolved in 200 mL of chloroform, and NBS (21.00 g, 0.12 mol) was added to the mixture for several portions. After the addition was complete, the reaction mixture was stirred for overnight and was then added to 300 mL of water. The organic was separated, and the water phase was extracted with chloroform (3 × 100 mL). The combined organics were washed

with brine (3 × 100 mL) and water (3 × 100 mL). The organics were dried over anhydrous $MgSO_4$. The solvent was removed in vacuo. The residue was purified with silica column chromatography and was eluted with light petroleum to yield **9** (21.60 g, 79.9%). EI *m/z*: = 466. ^{1}H NMR ($CDCl_3$, 400 MHz, δ): 2.67 (t, 4H), 1.65 (m, 4H), 1.32 (m, 12H), 0.88 (t, 6H). ^{13}C NMR (300 MHz, $CDCl_3$): 146.3, 141.3, 134.7, 84.0, 77.3, 31.6, 29.2, 24.9, 22.7, 14.2. Anal. Calcd for $C_{18}H_{26}S_2Br_2$: C, 46.35; H, 5.58; S, 13.73; Br, 34.33. Found: C, 46,30; H, 5.45; S, 13.66; Br, 34.28.

Synthesis of the Polymers. The synthesis of the polymers was carried out using palladium-catalyzed Stille-coupling between monomer 2,5-dibromo-3-hexylthiophene or **9** and (*E*)-1,2-bis(tributylstannyl)ethane, as shown in Scheme 3. All starting materials, reagents, and solvents were carefully purified, and all procedures were performed under an air-free environment. Under the protection of an argon atmosphere, monomer 2,5-dibromo-3-hexylthiophene or **9** (1 mmol) was dissolved in 10 mL of dried toluene, and (*E*)-1,2-bis(tributylstannyl)ethane (1 mmol) was added to the mixture. The solution was flushed with argon for 10 min, and 10 mg of Pd $(PPh_3)_4$ was added. After another flushing with argon for 20 min, the reactant was heated to reflux for 12 h. The terminal bromobenzene and benzene boronic acid were added as end cappers, with the bromobenzene added first and the benzene boronic acid added 12 h later. After stirring for another 12 h, the reaction solution was cooled to room temperature. The reaction mixture was added dropwise to 200 mL of methanol, filtered through a Soxhlet thimble, and then subjected to Soxhlet extraction with methanol, hexane, and chloroform. The polymer was recovered as a solid from the chloroform fraction by rotary evaporation. The polymer was purified with biobeads S-1 column chromatography eluted with THF, and the solvent was removed in vacuo. The solid was dried under vacuum for 1 day. The yields of the polymerization reactions were ~30−50%.

P3HTV. GPC: M_w = 28 K, M_n = 9.1 K, M_w/M_n = 3.08. ^{1}H NMR ($CDCl_3$, 400 MHz, δ): 7.13−6.67 (br, 3H), 2.59 (m, 2H), 1.58 (m, 2H), 1.34 (m, 6H), 0.87 (t, 3H). Anal. Calcd for $(C_{12}H_{16}S)_n$: C, 75.00; H, 8.33; S, 16.67. Found: C, 74.36; H, 8.21; S, 14.98.

DH-PTTV. GPC: M_w = 32 K, M_n = 28 K, M_w/M_n = 1.13. ^{1}H NMR ($CDCl_3$, 400 MHz, δ): 7.15−6.99 (br, 2H), 2.79 (m, 4H), 1.74 (m, 4H), 1.38 (m, 12H), 0.93 (t, 6H). Anal. Calcd for $(C_{20}H_{28}S_2)_n$: C, 72.29; H, 8.43; S, 19.28. Found: C, 72.18; H, 8.72; S, 18.96.

Acknowledgment. This work was supported by the NSFC (nos. 20574078, 20721061, 50633050, 60736004, and 50673093).

References and Notes

(1) Allard, S.; Forster, M.; Souharce, B.; Thiem, H.; Scherf, U. *Angew. Chem., Int. Ed.* **2008**, *47*, 4070.
(2) Ong, B. S.; Wu, Y. L.; Li, Y. N.; Liu, P.; Pan, H. L. *Chem. Eur. J.* **2008**, *14*, 4766.
(3) (a) Wang, Y.; Zhou, E. J.; Liu, Y. Q.; Xi, H. X.; Ye, S. H.; Wu, W. P.; Guo, Y. L.; Di, C. A.; Sun, Y. M.; Yu, G.; Li, Y. F. *Chem. Mater.* **2007**, *19*, 3361. (b) Zou, Y. P.; Wu, W. P.; Sang, G. Y.; Yang, Y.; Liu, Y. Q.; Li, Y. F. *Macromolecules* **2007**, *40*, 7231.
(4) Bao, Z. N.; Lovinger, A. J. *Chem. Mater.* **1999**, *11*, 2607.
(5) Li, Y. F.; Zou, Y. P. *Adv. Mater.* **2008**, *20*, 2952.
(6) Hou, J. H.; Tan, Z. A.; Yan, Y.; He, Y. J.; Yang, C. H.; Li, Y. F. *J. Am. Chem. Soc.* **2006**, *128*, 4911.
(7) Sun, X. B.; Zhou, Y. H.; Wu, W. C.; Liu, Y. Q.; Tian, W. J.; Yu, G.; Qiu, W. F.; Chen, S. Y.; Zhu, D. B. *J. Phys. Chem. B* **2006**, *110*, 7702.
(8) Huitema, H. E. A.; Gelinck, G. H.; Van der Putten, J. B. P. H.; Kuijk, K. E.; Hart, C. M.; Cantatore, E.; Herwig, P. T.; Van Breemen, A. J. J. M.; De Leeuw, D. M. *Nature* **2001**, *414*, 5–99.
(9) Huitema, H. E. A.; Gelinck, G. H.; Van der Putten, J. B. P. H.; Kuijk, K. E.; Hart, C. M.; Cantatore, E.; DeLeeuw, D. M. *Adv. Mater.* **2002**, *14*, 1201.
(10) Roncali, J. *Chem. Rev.* **1997**, *97*, 173.
(11) (a) Yamada, S.; Tokito, S.; Saito, S. *J. Chem. Soc., Chem. Commun.* **1987**, 1448. (b) Murase, I.; Ohnishi, T.; Noguchi, T.; Hirooka, M. *Polym. Commun.* **1987**, *28*, 229.
(12) (a) Gilch, H. G.; Wheelwright, W. L. *J. Polym. Sci.* **1966**, *4*, 1137. (b) Wessling, R. A.; Zimmerman, R. G.,U.S. Patent No 3401152, **1968**. (c) Wessling, R. A. *J. Polym. Sci., Part C: Polym. Lett.* **1985**, *72*, 55. (d) Son, S.; Dodabalapur, A.; Lovinger, A. J.; Galvin, M. E. *Science* **1995**, *269*, 376. (e) Louwet, F.; Vanderzande, D.; Gelan, J. *Synth. Met.* **1992**, *52*, 125. (f) Louwet, F.; Vanderzande, D.; Gelan, J. *Synth. Met.* **1995**, *69*, 509. (g) Louwet, F.; Vanderzande, D.; Gelan, J.; Mullens, J. *Macromolecules* **1995**, *28*, 1330.
(13) (a) Henckens, A.; Lutsen, L.; Vanderzande, D.; Knipper, M.; Manca, J.; Aernouts, T.; Poortsmans, J. *Proc. SPIE Int. Soc. Opt. Eng.* **2004**, *5464*, 52. (b) Gillissen, S.; Henckens, A.; Lutsen, L.; Vanderzande, D.; Gelan, J. *Synth. Met.* **2003**, *135−136*, 255.
(14) Prins, P.; Candeias, L. P.; van Breemen, A. J. J. M.; Sweelssem, J.; Herwig, P. T.; Schoo, H. F. M.; Siebbles, L. D. A. *Adv. Mater.* **2005**, *17*, 718.
(15) Fuchigami, H.; Tsumura, A.; Koezuka, H. *Appl. Phys. Lett.* **1993**, *63*, 1372.
(16) Smith, A. P.; Smith, R. R.; Taylor, B. E.; Durstock, M. F. *Chem. Mater.* **2004**, *16*, 4687.
(17) Hou, J. H.; Tan, Z. A.; He, Y. J.; Yang, C. H.; Li, Y. F. *Macromolecules* **2006**, *39*, 4657.
(18) Banishoeib, F.; Henckens, A.; Fourier, S.; Vanhooyland, G.; Breselge, M.; Manca, J.; Cleij, T. J.; Lutsen, L.; Vanderzande, D.; Nguyen, L. H.; Neugebauer, H.; Sariciftci, N. S. *Thin Solid Films* **2008**, *516*, 3978.
(19) McCulloch, I.; Heeney, M.; Bailey, C.; Genevicius, K.; Macdonald, I.; Shkunov, M.; Sparrowe, D.; Tierney, S.; Wagner, R.; Zhang, W. M.; Chabinyc, M. L.; Kline, R. J.; McGehee, M. D.; Toney, M. F. *Nat. Mater.* **2006**, *5*, 328.
(20) Lucas, L. A.; DeLongchamp, D. M.; Vogel, B. M.; Lin, E. K.; Fasolka, M. J.; Fischer, D. A.; McCulloch, I.; Heeney, M.; Jabbour, G. E. *Appl. Phys. Lett.* **2007**, *90*, 012112.
(21) Li, Y.; Wu, Y.; Liu, P.; Birau, M.; Pan, H.; Ong, B. S. *Adv. Mater.* **2006**, *18*, 3029.
(22) Rutherford, D. R.; Stille, J. K.; Elliott, C. M.; Reichert, V. R. *Macromolecules* **1992**, *25*, 2294.
(23) Taliani, C.; Zamboni, R.; Danieli, R.; Ostoja, P.; Porzio, W.; Lazzaroni, R.; Bredas, J. L. *Phys. Scr.* **1989**, *40*, 781.
(24) Danieli, R.; Taliani, C.; Zamboni, R.; Giro, G.; Biserni, M.; Mastragostino, M.; Testoni, A. *Synth. Met.* **1986**, *13*, 325.
(25) Miguel, L. S.; Matzger, A. J. *Macromolecules* **2007**, *40*, 9233.
(26) (a) Hou, J. H.; Huo, L. J.; He, C.; Yang, C. H.; Li, Y. F. *Macromolecules* **2006**, *39*, 594. (b) Hou, J. H.; Yang, C. H.; Li, Y. F. *Synth. Met.* **2005**, *153*, 93. (c) Zhou, E. J.; He, C.; Tan, Z. A.; Hou, J. H.; Yang, C. H.; Li, Y. F. *J. Polym. Sci., Part A: Poly. Chem.* **2006**, *44*, 4916.
(27) Prommerehne, J.; Vestweber, H.; Guss, W.; Mahrt, R. F.; Bassler, H.; Porsch, M.; Daub, J. *Adv. Mater.* **1995**, *7*, 551.
(28) Sun, Q. J.; Wang, H. Q.; Yang, C. H.; Li, Y. F. *J. Mater. Chem.* **2003**, *13*, 800.

MA801923C